Journal of Cellular Biochemistry 74:447–457 (1999)

Detection of Dendritic Cells in the Non-Obese Diabetic (NOD) Mouse Islet Pancreas Infiltrate Is Correlated With Th2-Cytokine Production

Gianpaolo Papaccio,[1]* **Antonio De Luca,**[2] **Bruno De Luca,**[3] **Francesco Aurelio Pisanti,**[4,5] **and Stefano Zarrilli**[6]

[1]Institute of Histology and Embryology, School of Medicine, Second University of Naples, 80138 Naples, Italy
[2]Laboratory for Cell Metabolism and Pharmacokinetics, Center for Experimental Research, Regina Elena Cancer Institute, 00158 Rome, Italy
[3]Institute of Topographical Anatomy, School of Medicine, Second University of Naples, Naples, Italy
[4]Department of Clinical Pathology, 80044 Ottaviano (Naples), Italy
[5]Department of Cell Biology, University of Calabria, 87036 Cosenza, Italy
[6]Department of Endocrinology, Molecular and Clinical Oncology, University of Naples Federico II, 80131 Naples, Italy

Abstract We investigate the role played by dendritic cells (DCs) in the non-obese diabetic (NOD) mouse pancreas. The early peri-islet, nondestructive infiltration phase, and intra-islet, destructive infiltration phase, which immediately precedes overt diabetes, are studied. Results show that infiltrating cells are Ia-b, ICAM-1, and, mainly, MIDC-8 immunoreactive (ir). These data from silica-treated animals and ultrastructural observations strongly support the hypothesis that DCs are both Ia-b-ir and ICAM-1-ir and that they exert a pivotal role during the period of early infiltration. This is a novel finding for NOD mice and increases the interest for this protective cell type during the rather complex islet infiltration process. Moreover, the cytokine profile demonstrates that Th2 protective cytokines are specific for peri-islet infiltrate. Disappearance of DCs from the infiltrate is concomitant with both the formation of intra-islet infiltration and the increase in proinflammatory Th1 cytokine levels. This further supports the hypothesis that DCs may exert a protective role against diabetes development. J. Cell. Biochem. 74:447–457, 1999.

Key words: dendritic cells; adhesion molecules; MIDC-8 immunoreactivity; Th1 and Th2 cytokines; NOD mice

In the non-obese diabetic (NOD) mouse, early infiltrating phenomena, such as peri-insulitis and peri-ductulitis, have been reported to be due mainly to recruited phagocytic monocytes and lymphocytes filling the postcapillary venules encircling the islets and the ductules [Papaccio et al., 1993]. However, the precise mechanisms regulating lymphocyte circulation within and between the islets, the exocrine portion of the gland, and other tissues remain poorly understood. It was recently suggested that the endothelium becomes activated and enhances mononuclear cell accumulation in the pancreas before the onset of type 1 diabetes in humans [Hänninen et al., 1992]. In fact, morphological alterations of the endothelium accompanying an increase in extravasation of mononuclear cells into the human pancreas have been observed [Hänninen et al., 1993]. Macrophages and lymphocytes have been found by many investigators to be the first, and/or major, elements in the inflammatory infiltrate to be involved in the anti-islet β-cell attack [Hänninen et al., 1992; Miyazaki et al. 1995; Kolb-Bachofen et al., 1988; Walker et al., 1988; Signore et al., 1989; Hayakawa et al., 1991]. In prediabetic Bio Breeding (BB) rats, insulitis begins with the accumulation of dendritic cells (DCs) at the periphery of some islets; then, when DCs form

Grant sponsor: Italian Ministry for University (MURST); Grant sponsor: Regional G.P. Campania Region; Grant number: L.R. 31.12.1994, n. 41; Grant sponsor: FIRC; Grant sponsor: CNR; Grant number: 96.02056.04.

*Correspondence to Gianpaolo Papaccio, Institute of Histology and Embryology, School of Medicine, Second University of Naples, 80138 Naples, Italy. E-mail: gpapacc@tin.it

Received 30 November 1998; Accepted 9 February 1999

clusters with infiltrating T lymphocytes, scavenger macrophages appear at the scene [Voorbij et al., 1989]. The role of these antigen-presenting DCs at the onset of the islet β-cell-specific autoimmune reaction has been stressed for this animal model of type 1 diabetes. In addition, extra-islet infiltration is a very early and typical phenomenon involving ducts and exocrine septa in the NOD mouse [Hänninen et al., 1993]. Moreover, peri-islet and intra-islet infiltration are now viewed differently, the former being thought of as a "protective" phenomenon and the latter being a "destructive" one [Shedaheh et al., 1993; Muir et al., 1995]. Understanding how and where one phenomenon leads to the other would be important in the understanding of the anti-islet β-cell attack. The elements taking part in this point of passage of the islet inflammatory infiltration have not been identified as yet.

The aim of this study was to investigate the infiltrating cells during both the early and late periods of infiltration (i.e., during the nondestructive and destructive periods) within the islets and the exocrine portion of NOD pancreas, in an effort to determine the role of dendritic cells in NOD, using methods that facilitate the detection of these cells, including specific monoclonal antibodies and treatment with silica particles (see under Materials and Methods).

MATERIALS AND METHODS

Animals

NOD mice originally purchased from Bommice (Denmark) and bred in our facility, free from viral infections, fed ad libitum and weighing 18–32 g, were used. In this colony, approximately 90% of females become diabetic and present with peri-vasculitis at about 5 weeks of age and with peri-insulitis with extra-islet infiltration (nondestructive lesions) at around 10 weeks of age. Destructive intra-islet infiltration is detectable by weeks 12–15. Clinical signs of diabetes are observable about 10 weeks later. Only a small fraction (10%) of male NOD mice become diabetic, but at least 60% of these mice show a peri-insulitis and other signs of infiltration that do not progress to intra-islet infiltration and diabetes.

Glycemia

Blood glucose levels were tested weekly using the hexokinase method (Boehringer, Mannheim, Germany). Animals were considered hyperglycemic when their nonfasting blood glucose levels were >8 mmol/L, but <12 mmol/L, in two successive determinations. Mice were considered diabetic when their blood glucose levels exceeded 12 mmol/L.

Treatment With Silica

Five-week-old female NOD mice (n = 30) were treated intraperitoneally with silica (Sigma, St. Louis, MO) every fifth day (200 mg/kg body weight) for 30 days and killed at week 10 (n = 10), 15 (n = 10), or 20 (n = 10) (silica-treated group). This treatment clears phagocytes and makes the detection of DCs easier [Charlton et al., 1988]. Vehicle-only treated 10-week-old (n = 10 males and n = 10 females), 15-week-old (n = 10 males and n = 10 females), and 20-week-old (n = 10 males and n = 10 females) NOD mice (control NOD group), and 12 C57Bl6/J (n = 6 males and n = 6 females) mice of the same ages served as controls. At sacrifice, animals were anesthetized under ether and the pancreas of the female mice removed and processed for morphology and cytochemistry.

General Morphology

Samples were fixed in Bouin's solution and embedded in paraffin for light microscopy. Serial sections (5 μm thick) were stained with hematoxylin & eosin (H&E) for general morphology. For the semiquantitative evaluation of infiltration, only sections containing six or more islets were selected and at least 50 islets per pancreas were evaluated. The degree of inflammatory infiltration was scored from 0 to 5 as follows: score 1 (infiltrates in small foci at the islet periphery); score 2 (infiltrates surrounding the islets (peri-insulitis); score 3 (intra-islet infiltration <0% of the islet, without islet derangement); score 4 (extensive infiltration, 50% of the islet, cell destruction and prominent cytoarchitectural derangement); and score 5 (islet atrophy because of β-cell loss).

The evaluation was carried out by two different researchers. A third researcher scored the slides without knowing the group origin of the slides.

Criteria for DC identification at this level are summarized in Table I.

TABLE I. Criteria for Morphological Identification of Dendritic Cells

Light microscopy
Presence of cytoplasmic processes
Reniform and eccentrically positioned nucleus
Strong Ia–b immunoreactivity
Not positive for CD3, CD4, CD8, or macrophage antibodies
Transmission electron microscopy
Relatively electrolucent cytoplasm
Blunt processes generally devoid of organelles
Smooth-surfaced vesicles (lysosomes) of various aspect, generally of small dimensions
Eccentric, irregularly shaped nucleus, lined with a rim of heterochromatin

Modified after Voorbji et al. [1989] and Setum et al. [1993].

Immunocytochemistry

Tissue from the tail of the pancreas from each animal was frozen and cryosectioned. Sections were stained by the avidin-biotin peroxidase indirect staining method [Papaccio et al., 1991]. Dendritic cells have been shown to be positive for both Ia-b and ICAM-1 molecules [Steinman, 1991]. The other antibodies were used to detect dendritic cells specifically (MIDC-8 is a very specific cytoplasmic component and is absent from thymocytes and Langerhans cells) or to differentiate dendritic cells from lymphocytes and macrophages because DCs are not actively phagocytic and do not express T-lymphocyte-specific or macrophage-specific antigens [Austyn, 1987]. Therefore, monoclonal antibodies used in this experiment were: anti-Ia-b (IgG_1; Dakopatts, Milan, Italy); anti-ICAM-1 rat anti-mouse (Medac, Hamburg, Germany); anti-mouse dendritic cells MIDC-8 (rat IgG_{2a}; BMA Biomedicals AG, Augst, Switzerland); anti-T lymphocyte (Dakopatts, Milan, Italy) CD3 (T3–4B5), CD4 (MT310), and CD8 (DK24); anti-macrophage antibody EBM 11 (Dakopatts, Milan, Italy). The secondary antibody was biotinylated goat anti-rat antibody. Anti-Ia-b antibody was used because MHC class II antigens are known to play a role in initiating the immune response [Bluacerraf and Germain, 1987], and Ia-b immunoreactive cells have been found in islets of Langerhans in the early phase of infiltration [Papaccio et al., 1991]. Intercellular adhesion molecule-1 (ICAM-1) is an adhesion molecule belonging to the immunoglobulin superfamily and binds to endothelial cells and cells involved in the adherence and emigration processes [Springer, 1990].

Semiquantitative analysis was performed also. At least 30 sections (5 μm thick) per animal were observed, and the immunoreactive elements were noted on alternate sections, using the M4 Image Analysis System (Image-Brock University, St. Catherine, Ontario, Canada). Data were expressed as a percentage of positive-stained cells per section ±SD. When pertinent, statistical analyses were performed (see below).

Ultrastructure

Small cubes of pancreatic tail were fixed in 2.5% glutaraldehyde in a 0.1 M phosphate buffer, postfixed in 0.1% OsO_4 in the same buffered solution for 1 h, then dehydrated and embedded in epoxy resins. Counterstained (uranyl acetate and lead citrate) ultrathin sections were observed under an electron microscope (Zeiss EM 109, Germany). Criteria for DC identification at this level are summarized in Table I.

Cytokine Profile

Islets (500 per dish) belonging to untreated male and female NOD animals (10, 15, and 20 weeks old) were obtained from pancreas using standard procedures and centrifuged to a pellet (200g, 2 min), the supernatant removed, and used for measurement of Th1 proinflammatory cytokines, including interleukin-2 (IL-2), interferon-γ (IFN-γ), and tumor necrosis factor-α (TNF-α), and protective Th2 cytokines, including IL-4 and IL-10 levels after centrifugation for 5 min at 2,000 rpm to eliminate cell debris. The concentrations of IL-2, IFN-γ, TNF-α, IL-4, and IL-10 were measured by enzyme-linked immunosorbent assay (ELISA) using monoclonal antibodies specific for IL-2, IFN-γ, TNF-α, IL-4, and IL-10 [Openshaw et al., 1995]. The amount of cytokine present was determined from the standard curves from purified recombinant cytokines. Values are expressed as U/ml.

Statistical Analysis

Student's *t*-test (level of significance set at $P < 0.05$) and analysis of variance (ANOVA 1) were used.

RESULTS

Glycemia

The results of the experiments are summarized in Table II. Silica-treated NOD mice, un-

TABLE II. Blood Glucose Levels[a]

Group	Week 5	Week 10	Week 15	Week 20	Week 25
NOD silica-treated					
Females	5.5 ± 0.3	5.5 ± 0.5	5.8 ± 1.0	6.2 ± 0.8	6.0 ± 1.0
NOD controls					
Females	5.7 ± 0.9	5.0 ± 1.0	7.7 ± 1.1	19.1 ± 3.0	24.0 ± 4.5
Males	5.0 ± 0.4	5.0 ± 0.5	5.2 ± 0.6	5.8 ± 0.6	5.9 ± 0.8
C57BL6/J controls					
Females	4.9 ± 0.4	5.0 ± 0.5	5.7 ± 0.5	5.9 ± 0.9	5.3 ± 1.0
Males	5.0 ± 0.2	5.7 ± 0.6	5.3 ± 0.5	4.9 ± 0.3	5.2 ± 0.9

NOD, non-obese diabetic.
[a]Values, expressed in mmol/L, are given as mean ± SD.

TABLE III. Mean of Insulitis Grading Scores

	Week 10	Week 15	Week 20
C57BL6/J	0	0	0
NOD controls (female)	2.1	3.7	4.6
NOD controls (male)	1.4[a]	2.0[b]	2.0[b]
NOD silica-treated	0.5[c]	0.5[c]	0.9

NOD, non-obese diabetic.
[a]Six of 10 animals.
[b]Eight of 10 animals.
[c]Nine of 10 animals.

treated male NOD animals and C57Bl6/J mice showed normal glycemic levels throughout the experiment. Glycemic levels of 15-week-old control female NOD mice were significantly higher as compared with the others ($P < 0.01$), with values close to 8 mmol/L. Blood glucose levels of 20-week-old control female NOD mice were further increased exceeding 12 mmol/L and animals were considered overtly diabetic.

Standard Light Microscopy

The means of insulitis grading scores are summarized in Table III. Islets of control 10-week-old female NOD mice either were normal or showed only few infiltrating cells at the periphery, mainly in the vicinity of a nearby duct (mean score = 2.1). Male NOD animals of the same age showed identical pancreatic lesions, but these findings were limited to 6 of 10 animals (mean score 1.4). Islets from 8 of 10 silica-treated NOD mice killed at week 10 were not infiltrated (mean score = 0.5), and the remaining two animals showed infiltration limited to the islet periphery, usually near a duct (mean score = 1.0). Fifteen-week-old female NOD mice were infiltrated massively and exhibited an intra-islet infiltration with several instances of destructive infiltration with cytoarchitectural derangement (mean score = 3.7), as well as duct infiltration and small foci of exocrine parenchyma infiltration. Twenty-week-old control NOD females showed a limited number of massively infiltrated islets because most were atrophic and retracted due to cell loss (mean score = 4.6).

Eight of 10 NOD 15-week-old male animals showed a peri-islet infiltration (nondestructive lesion) with duct infiltration (mean score = 2.0); in the remaining male animals, islets were not infiltrated. The same pattern was observed in 20-week-old male NOD controls. Islets from 9 of 10 silica-treated NOD mice killed at week 15 were not significantly infiltrated (mean score = 0.9). The remaining animal showed infiltrated islets (mean score = 2.5). At week 20, silica-treated animals showed non infiltrated islets or islets with small foci of infiltration (mean score = 0.8). Infiltration was not encountered in any pancreatic sections from C57Bl6/J controls.

Immunohistochemistry

Ten-week-old control NOD mice. Ia-b-immunoreactive (ir) elements were seen at the islet periphery or, less frequently, within the islet parenchyma (Fig. 1a). In addition, cells of the epithelium and of the connective layer of pancreatic ducts, as well as peri-islet cells (islet capsule), and scattered extra-islet cells seen along the septa, were also Ia-b-ir. ICAM-1 immunoreactivity was also found at the islet periphery. Small clusters and scattered cells (Fig. 1b) found along septa and within the exocrine parenchyma also were ICAM-1-ir. These cells seemed to belong to the dendritic cell lineage because of their location, shape, and eccentrically positioned nucleus.

Cells staining positive for MIDC-8 (Fig. 1c), which demonstrated that they belonged to the

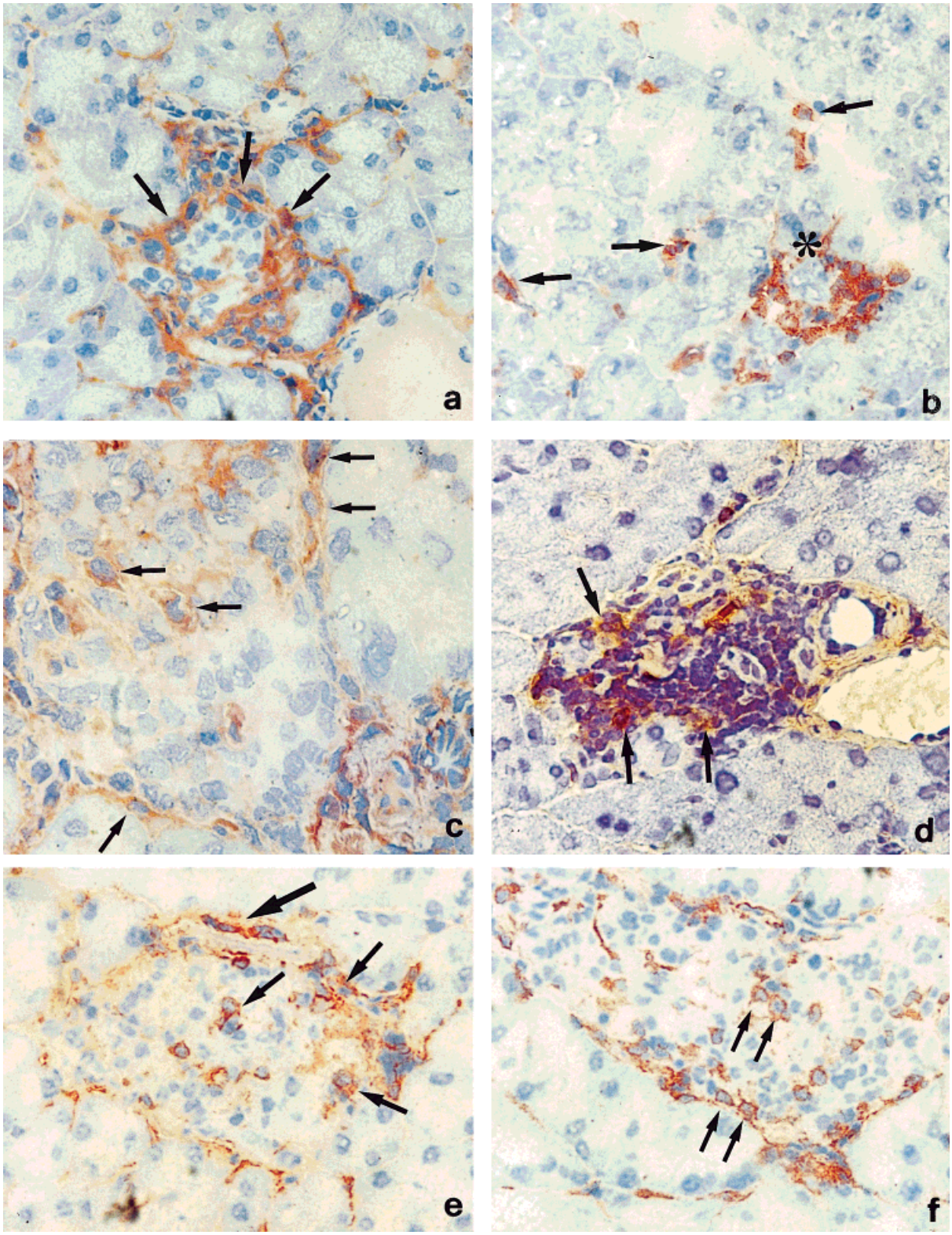

Fig. 1. **a:** Light micrograph of an untreated 10-week-old female non-obese diabetic (NOD) mouse showing Ia-b immunoreactive elements, located mainly at the islet periphery (arrows). ×300. **b:** Light micrograph of an untreated 10-week-old female NOD mouse showing ICAM-1 immunoreactive elements in small clusters (asterisk) or scattered within the exocrine parenchyma (arrows). Many of these cells show a dendritic shape and an eccentric nucleus. ×300. **c:** Light micrograph of an untreated 10-week-old female NOD mouse showing MIDC-8 immunoreactive elements at the islet level (arrows). ×450. **d:** Light micrograph of an untreated 10-week-old female NOD mouse showing EBM-11 immunoreactive elements at the islet periphery (arrows). ×450. **e:** Light micrograph of a silica-treated 15-week-old female NOD mouse, showing ICAM-1 immunoreactive cells at the islet level (arrows). Note that endothelia of peri-islet vessels also show ICAM-1 positivity (thick arrow). ×300. **f:** Light micrograph of a silica-treated 15-week-old female NOD mouse, showing MIDC-8 immunoreactive cells at the islet level (arrows). Endothelia do not show immunoreactivity. ×300.

dendritic cell lineage, were most probably Ia-b-ir and ICAM-1-ir because they were in similar locations and had the same shape and morphology as the latter. Moreover those elements did not show immunoreactivity for CD3, CD4, or CD8, which, in turn, confirmed that they did not belong to the T-lymphocyte lineage. A weak EBM-11 immunoreactivity was seen mainly at the islet periphery (Fig. 1d) and less frequently within the exocrine parenchyma. This pattern was seen in all females and in 6 of 10 male animals. The remaining male animals did not exhibit significant immunoreactivity.

Semiquantitative evaluation (Table IV) demonstrated that islet Ia-b-ir cells were significantly more numerous than islet ICAM-1-ir elements ($P < 0.001$). By contrast, extra-islet Ia-b-ir elements were significantly less numerous than extra-islet ICAM-1-ir cells ($P < 0.001$). Moreover, within the islets, MIDC-8-ir cells were significantly less numerous than Ia-b-ir cells ($P > 0.001$), only slightly less numerous than ICAM-1-ir cells, but significantly more numerous than EBM-11-ir cells ($P > 0.001$). The numbers of extra-islet MIDC-8-ir and ICAM-1-ir elements were similar.

Fifteen-week-old control NOD mice. These animals showed considerably different sex-related features. Females showed a reduced Ia-b immunoreactivity in both intra- and extra-islet compartments as compared with 10-week-old animals ($P > 0.0001$). ICAM-1 expression was slightly lower in intensity, within the islet but almost unmodified in the extra-islet portion of the gland. Moreover, ICAM-1 immunoreactivity was always greater than that of Ia-b molecules ($P < 0.0001$) in the exocrine pancreas. Islet MIDC-8-ir cells were noted in extremely small numbers and extra-islet MIDC-8-ir elements were often undetectable ($P > 0.0001$ vs 10-week-old animals). CD8 and CD4 immunoreactivities often were observed around and within the islets, with a prevalence of CD8-ir cells ($P < 0.001$ vs CD4-ir elements), while CD3-ir cells were only scarcely observed. EBM-11 immunoreactivity was observed scattered within the islets and the exocrine pancreas.

Male animals however showed the same pattern observed in 10-week-old females (8/10 animals), i.e., a peri-islet infiltration with Ia-b-ir, ICAM-1-ir, and MIDC-8-ir cells. The remaining 2 of 10 male animals did not show any immunoreactivities (data from male animals are not shown).

Twenty-week-old control NOD mice. In female NOD animals, Ia-b-ir, EBM-11-ir and MIDC-8-ir elements were not observed. ICAM-1-ir elements were observed mainly in extra-islet locations (ducts, septa, and endothelia), though of lower intensity with respect to 10- and 15-week-old animals ($P < 0.01$). CD8 or CD4 immunoreactivities were sometimes observed around and within the islets, with a prevalence of CD8-ir cells ($P < 0.01$ vs CD4-ir elements). Conversely, male animals still showed the same pattern observed in 10-week-old females (8 of 10 animals) (not shown), and the remaining 2/10 mice did not show any immunoreactivity.

Silica-treated NOD mice. Ia-b-ir elements were observed at the islet periphery and along septa in the exocrine portion of the gland in 10-week-old, in 15-week-old, and in 20-week-

TABLE IV. Quantitative Evaluation of the Immunoidentity of Cells Surrounding and Infiltrating the Islets and of Cells in the Exocrine Pancreas (Excluding Vessels and Ductules) of Untreated Female NOD Mice[a]

	Islets			Pancreas		
Antibody	Week 10	Week 15	Week 20	Week 10	Week 15	Week 20
Ia–b	23.0 ± 2.0	7.5 ± 0.7	0.2 ± 0.1	10.4 ± 1.0	4.3 ± 0.5	0.5 ± 0.1
ICAM-1	13.6 ± 1.1	9.5 ± 0.8	2.0 ± 0.5	16.5 ± 1.6	12.9 ± 0.8	7.5 ± 1.2
MIDC-8	10.9 ± 1.4	2.0 ± 0.5	0.2 ± 0.1	15.0 ± 1.2	0.6 ± 0.5	0.2 ± 0.1
EBM-11	4.7 ± 0.9	2.0 ± 0.7	0.2 ± 0.1	2.3 ± 0.6	0.7 ± 0.6	0.2 ± 0.1
CD3	0.2 ± 0.1	2.3 ± 0.4	0.2 ± 0.1	0.1 ± 0.1	0.1 ± 0.1	0.1 ± 0.1
CD4	0.2 ± 0.1	5.3 ± 0.4	2.0 ± 0.5	0.1 ± 0.1	0.1 ± 0.1	0.1 ± 0.1
CD8	0.2 ± 0.1	10.3 ± 1.5	3.5 ± 1.0	0.1 ± 0.1	0.1 ± 0.1	0.1 ± 0.1

NOD, non-obese diabetic.

[a]Data are expressed as a percentage of positive cells per section. Data belonging to male mice are not given (see the text). Data belonging to C57B16/J controls also not given because they are completely negative.

old silica-treated female mice (Table V). Their numbers were significantly lower when compared with those found in untreated NOD animals ($P < 0.001$). ICAM-1-ir (Fig. 1e) cell numbers were only slightly decreased within the islets and in the exocrine pancreas. Moreover, a relevant number of peri- and intra-islet infiltrating elements, as well as of elements located along septa within the exocrine portion of the gland, were MIDC-8-ir (i.e., dendritic cells) (Fig. 1f). Of particular interest is the finding that, after silica treatment, EBM-11-ir cells were cleared completely while exocrine ICAM-1-ir cells, as well as dendritic cells (MIDC-8-ir elements) did not change in 15-week-old and 20-week-old animals. Therefore, silica depleted the

TABLE V. Quantitative Evaluation of the Immunoidentity of Cells Surrounding and Infiltrating the Islets and of Cells in the Exocrine Pancreas (Excluding Vessels and Ductules) of Silica-Treated Female NOD Mice[a]

	Islets			Pancreas		
Antibody	Week 10	Week 15	Week 20	Week 10	Week 15	Week 20
Ia–b	9.0 ± 2.6	5.9 ± 1.6	5.5 ± 1.6	5.6 ± 0.5	3.1 ± 0.6	3.0 ± 0.5
ICAM-1	9.0 ± 0.7	7.7 ± 0.5	7.5 ± 0.5	7.7 ± 0.7	9.2 ± 1.6	8.0 ± 1.2
MIDC-8	9.7 ± 1.2	7.3 ± 0.8	7.0 ± 1.0	9.5 ± 0.7	8.5 ± 0.5	8.0 ± 1.0
EBM-11	0.2 ± 0.1	0.1 ± 0.1	0.1 ± 0.1	0.2 ± 0.1	0.1 ± 0.1	0.1 ± 0.1

NOD, nonobese diabetics.
[a]Data are expressed as a percentage of positive cells per section.

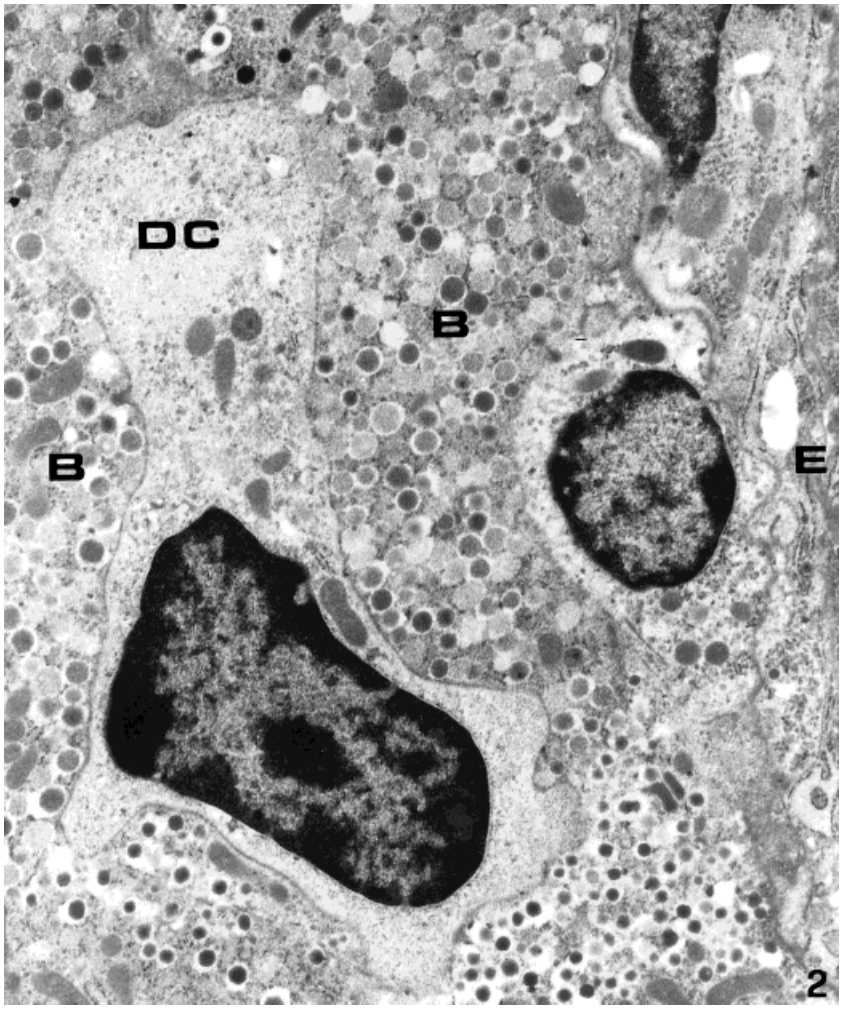

Fig. 2. Transmission electron micrograph of a silica-treated 15-week-old non-obese diabetic (NOD) mouse showing a dendritic cell at the islet periphery, surrounded by islet cells. The dendritic cell shows blunt processes devoid of organelles, an eccentric nucleus with a rim of heterochromatin and lysosomes. DC, dendritic cell; B, islet cell; E, exocrine cell). ×7,000.

pancreatic content of macrophages and other phagocytes, and the remaining immunoreactive cells were DCs. The above-described pattern did not change during the experiment.

C57Bl6/J controls. Islets and exocrine pancreas were negative for all antibodies in these controls.

Ultrastructure

In untreated 10-week-old female NOD mice and in 60% of male animals of the same age, marginated mononuclear phagocytes were observed within the lumen of the venules surrounding the islets as well as in sinusoids within the islet parenchyma. Marginated plasma cells also were seen. Islet cell damage or morphological changes of the endothelium were not observed, and intraislet vessels did not show significant alterations. Marginating elements were observed only occasionally in silica-treated NOD mice.

In both 10-week-old untreated (females and 60% of males) and silica-treated NOD female mice, irregularly shaped cells with blunt protrusions (generally devoid of organelles), and a reniform, eccentrically positioned nucleus lined with a rim of heterochromatin were observed both at the islet periphery (Figs. 2, 3) and along the septa in the exocrine parenchyma. Their relatively electrolucent cytoplasm contained mitochondria, short slips of rough and smooth endoplasmic reticulum, a well-developed Golgi apparatus, abundant smooth-surfaced vesicles, and scattered free ribosomes. Because of their morphological appearance, these cells belonged to the dendritic cellular stem (Table I).

In 15-week-old untreated NOD females, islet β cells often were surrounded by numerous infiltrating elements which were mainly lymphocytes. Several macrophages also were seen phagocytosing islet β cells, whose cytoplasm often showed signs of sufferance. Dendritic cells were never observed. Conversely, islets belonging to male animals of the same age did not show a progression of the lesions. The aspect was very close to that observed in 10-week-old animals and dendritic cells often were noted both at the islet periphery or among the exocrine parenchyma.

In 20-week-old control NOD females, islets were of small dimensions and insulin-containing cells were not encountered. Infiltrating elements were not present, with few exceptions. Islets of male animals and islets of silica-treated NOD female animals showed the same aspect observed in 10-week-old male and silica-treated animals. C57Bl6/J controls and 60% of male NOD mice did not show pancreatic lesions.

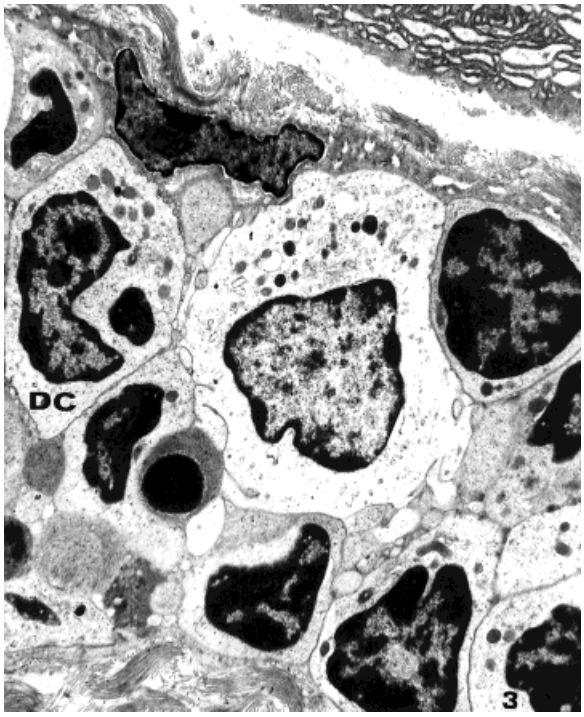

Fig. 3. Transmission electron micrograph of an untreated 15-week-old non-obese diabetic (NOD) mouse showing a dendritic cell among other infiltrating cells, mainly lymphocytes, at the islet periphery. The dendritic cell (DC) shows an eccentrically positioned reniform nucleus, lined with a rim of heterochromatin, and cytoplasmic lysosomes. ×5,000.

Cytokine Profile

Th2 protective cytokines are correlated with the initial peri-insulitis phase (10 weeks) when mainly IL-4 and IL-10 cytokines are detected in NOD female and male controls (Fig. 4). Levels of Th2 protective cytokines decrease significantly ($P < 0.001$) during the intra-islet infiltration period (15 weeks) in untreated NOD females, and concomitantly, in these animals, Th1 proinflammatory cytokine levels significantly increased ($P < 0.001$) up to week 20. In untreated male NOD animals, the Th2 levels remain unaltered and were constantly higher with respect to Th1, mirroring the persistence of the peri-islet lesion in these animals, which does not progress toward the destructive lesion seen at week 20.

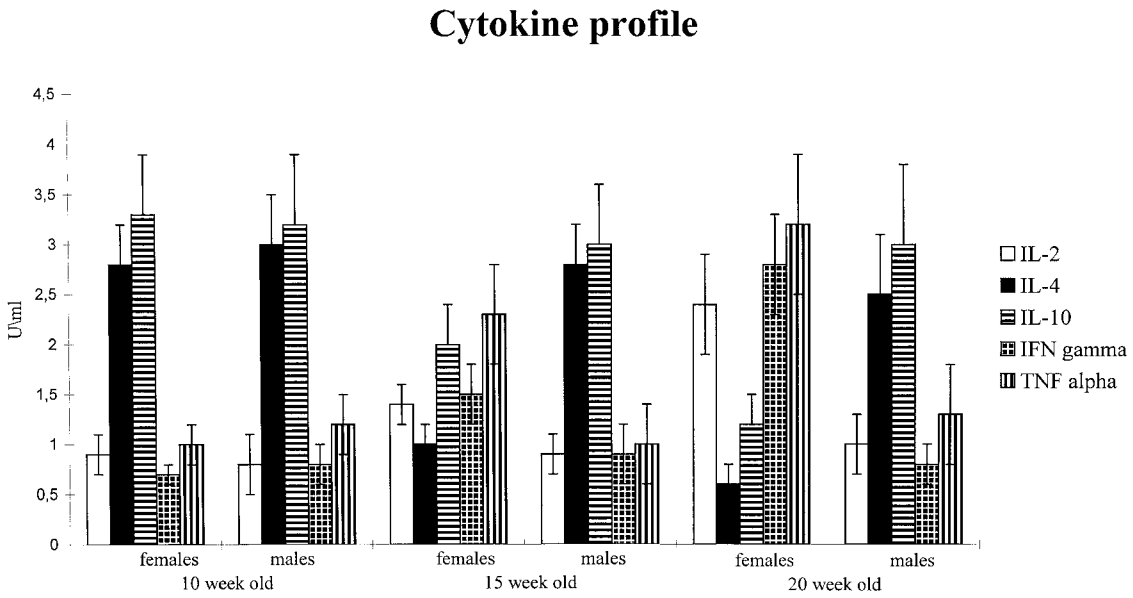

Fig. 4. Cytokine profile of untreated female and male non-obese diabetic (NO)D animals. Values are expressed as U/ml.

DISCUSSION

In this study, we show that, at a very early stage of autoimmune infiltration in NOD mice, a rather consistent number of cells seen both at the islet periphery and along septa in the exocrine pancreas show Ia-b, ICAM-1, and MIDC-8 immunoreactivities. Only slight EBM-11 (macrophage) immunoreactivity, as well as absence of immunoreactivity for CD3, CD4, or CD8 antibodies, are seen. These data, taken together with the morphological and ultrastructural appearance, strongly support the hypothesis that dendritic cells are both Ia-b and ICAM-1-ir and that these elements exert a role during the nondestructive period of infiltration. This is a novel finding for NOD mice.Treatment with silica particles, which can clear phagocytes, has reinforced this hypothesis because Ia-b-ir cell numbers were significantly lower when compared with those found in untreated NOD animals ($P < 0.001$). ICAM-1-ir cell numbers are decreased only slightly both within the islets and in the exocrine pancreas. Moreover, after silica treatment, EBM-11-ir cells are completely cleared, ruling out the possibility that immunoreactive elements are macrophages and that this may explain the decrease in Ia-b-ir cell numbers. The difference between extraislet Ia-b-ir and ICAM-1-ir cell numbers is explained by the fact that fibroblasts and other elements of connective tissue also express ICAM-1 molecules [Dustin et al., 1986].

The cytokine profile confirms that during the peri-islet infiltrate period, in untreated NOD females high levels of Th2 protective cytokines are observed, but during the intra-islet infiltrate mainly Th1 proinflammatory cytokines are produced. Therefore, this pattern demonstrates that, when DCs are present (i.e., during the peri-islet lesion), Th2 protective cytokines continue to be produced but, when the intra-islet lesion takes over, DCs disappear from the scene and Th1 proinflammatory cytokines are prevailingly produced within the islets thus giving further support to a possible protective role exerted by DCs. Moreover, in untreated male animals, whose islets are surrounded by a peri-islet infiltrate which, in most cases, does not progress further, Th2 protective cytokines are prevailingly detected and DCs do not disappear from the scene, lending support to the hypothesis of a possible role of immunosurveillance exerted by these cells.

DCs are potent antigen-presenting cells for a variety of immune responses but their mechanism of action has not been well established yet. It is known that DCs accumulate at sites of infection or inflammation and can physically cluster with lymphocytes and with other DCs independent of MHC specificity [Inaba et al., 1984; Green and Jotte, 1985]. A striking feature of DCs is their constitutive expression of high levels of surface MHC class II antigens [Setum et al., 1993], which is confirmed in this study. In

previous studies [Papaccio et al., 1994], it was demonstrated that infiltration occurring in NOD mice is a rather extensive and non specific process and which later undergoes a restriction. DCs showed strong Ia-b-ir and ICAM-1 immunoreactivities also in the exocrine portion of the gland, along septa, or in small clusters within it. This particular location provides further evidence that the whole pancreas is involved in the autoimmune process during the early stage of the disease. It was recently hypothesized [Amano et al., 1995] that islet-specific $CD8^+$ cells are needed initially to open a window into the islets with the help of $CD4^+$ cells specifically reactive to islet cells. Then, the homing of non-specific or specific $CD8^+$ and $CD4^+$ T cells into the islets would occur in context with certain homing ligand (i.e., ICAM-1) interaction. Finally, $CD8^+$ T cells are also required for the development of overt diabetes by the direct destruction of cells in NOD mice [Amano et al., 1995]. These steps, in view of the findings in this study, seem to require the disappearance of DCs from the scene, and the persistence of ICAM-1-ir elements, which have been shown to remain even when overt diabetes occurs [Papaccio et al., 1998].

ACKNOWLEDGMENTS

The authors gratefully thank Giuseppe Falcone (Histology Department, University Federico II, Naples, Italy) and Georgios Daphnys (Zoological Station, Naples, Italy) for expert technical help. This work has been supported by MURST (Italian Ministry for University) (60%) and Regional (G.P.-Campania Region, L.R. 31.12.1994, n. 41), grant. A.D.L. is the recipient of an FIRC grant. Professor Damiano Zaccheo (School of Medicine, DIMES, Section of Human Anatomy, University of Genova) is kindly acknowledged for help and criticism and for CNR grant 96.02056.04.

REFERENCES

Amano K, Yokono K, Hasegawa Y, Taki T, Tomnaga Y, Yoneda R, Nagata M, Kasuga M. 1995. A novel function of islet-derived $CD8^+$ T cells in initiating and developing autoimune insulin-dependent diabetes mellitus in non-obese diabetic (NOD) mice. Diabetes Res Clin Pract 28: 161–172.

Austyn JM. 1987. Lymphoid dendritic cells. Immunology 62:161–170.

Bluacerraf B, Germain RN. 1987. The immune genes of the major histocompatibility complex. Immunol Rev 38:70–119.

Charlton B, Bacelji JA, Mandel T. 1988. Administration of silica particles or anti-LyT2 antibody prevents B cell destruction in NOD mice given cyclophosphamide. Diabetes 37:930–935.

Dustin ML, Rothlein R, Bahn AK, Dinarello CA, Springer TA. 1986. Induction by IL-1 and interferon-gamma: tissue distribution, biochemistry and function of natural adherence molecule (ICAM-1). J Immunol 137:245–254.

Green J, Jotte R. 1985. Interactions between T helper cells and dendritic cells during the rat mixed leukocyte reaction. J Exp Med 162:1546–1560.

Hänninen A, Jalkanen S, Salmi M, Toikkanen S, Nokolakaros G, Simell O. 1992. Macrophages, T-cell receptor usage and endothelial cell activation in the pancreas at the onset of insulin-dependent diabetes. J Clin Invest 90: 1901–1910.

Hänninen A, Salmi M, Simell O, Jalkanen S. 1993. Endothelial cell-binding properties of lymphocytes infiltrated into human diabetic pancreas. Implications for pathogenesis of IDDM. Diabetes 42:1656–1662.

Hayakawa M, Yokono K, Nagata M, Hatamori N, Ogawa W, Miki A, Mizoguti H, Baba S. 1991. Morphological analysis of selective destruction of pancreatic B cells by cytotoxic T lymphocytes in NOD mice. Diabetes 40:1210–1216.

Inaba K, Steinman RM. 1984. Resting and sensitized T lymphocytes exhibit distinct stimulatory (antigen presenting cell) requirements for growth and lymphokine release. J Exp Med 160:1717–1725.

Kolb-Bachofen V, Epstein S, Kiesel U, Kolb H. 1988. Low-dose streptozocin-induced diabetes in mice. Electron microscopy reveals single cell insulitis before diabetes onset. Diabetes 37:21–27.

Miyazaki A, Hanafusa T, Yamada K, Miyagawa J, Fujino-Kurihara H, Nakaijma H, Nonata K, Tarni S. 1985. Predominants of T lymphocytes in pancreatic islets and spleen of pre-diabetic nonobese diabetic (NOD) mice: a longitudinal study. Clin Exp Immunol 60:622–630.

Muir A, Peck A, Clare-Salzler M, Song Y-H, Cornelius J, Luchetta R, Krischer J, Maclaren N. 1995. Insulin immunization of NOD mice induces a protective insulitis characterized by diminished intraislet interferon transcription. J Clin Invest 95:628–634.

Openshaw P, Murphy EE, Hosken NA, Maino V, Davis K, Murphy K, O'Garra A. 1995. Heterogeneity of intracellular cytokine synthesis at the single-cell level in polarized T helper 1 and T helper 2 populations. J Exp Med 182: 1357–1367

Papaccio G, Chieffi Baccari G, Mezzogiorno V, Esposito V. 1993. Extraislet infiltration in NOD mouse pancreas: observations after immunomodulation. Pancreas 8:459–464.

Papaccio G, Chieffi Baccari G, Strate C, Linn T. 1994. Pancreatic duct inflammatory infiltration in the non obese diabetic (NOD) mouse. J Anat 185:465–470.

Papaccio G, Latronico MGV, Pisanti FA, Federlin K, Linn T. 1998. Adhesion molecules and microvascular changes in the nonobese diabetic (NOD) mouse pancreas. An NO-inhibitor ($_L$-NAME) is unable to block adhesion inflammation-induced activation. Autoimmunity 27:65–77.

Papaccio G, Linn T, Federlin K, Volkman A, Esposito V, Mezzogiorno V. 1991. Further morphological and biochemical observations on early low-dose streptozocin diabetes in mice. Pancreas 6:659–667.

Setum CM, Serie JR, Hegre OD. 1993. Dendritic cell/lymphocyte clustering: morphologic analysis by transmission electron microscopy and distribution of gold-labeled MHC class II antigens by high resolution scanning electron microscopy. Anat Rec 235:285–295.

Shehadeh NN, LaRosa F, Lafferty KJ. 1993. Altered cytokine activity in adjuvant inhibition of autoimmune diabetes. Autoimmunity 6:291–300.

Signore A, Pozzilli P, Gale EAM, Andreani D, Beverly PCL. 1989. The natural history of lymphocyte subsets infiltrating the pancreas of NOD mice. Diabetologia 32:282–289.

Springer TA. 1990. Adhesion receptors of the immune system. Nature 346:425–434.

Steinman RM. 1991. The dendritic cell system and its role in immunogenicity. Annu Rev Immunol 9:271–296.

Voorbij HAM, Jeucken PHM, Kabel PJ, De Haan M, Drexhage HA. 1989. Dendritic cells and scavenger macrophages in pancreatic islets of prediabetic BB rats. Diabetes 38:1623–1629.

Walker R, Bone AJ, Cooke A, Baird JD. 1988. Distinct macrophage subpopulation in pancreas of pre-diabetic BB/E rats: possible role for macrophages in pathogenesis of IDDM. Diabetes 37:1301–1304.